Gravity waves in the arctic mesosphere during the MaCWAVE/MIDAS summer rocket program

B. P. Williams,[1,2] D. C. Fritts,[1] L. Wang,[1] C. Y. She,[3] J. D. Vance,[3] F. J. Schmidlin,[4] R. A. Goldberg,[5] A. Müllemann,[6] and F.-J. Lübken[6]

Received 21 March 2004; revised 31 July 2004; accepted 11 October 2004; published 9 November 2004.

[1] The MaCWAVE/MIDAS rocket campaign occurred at the Andøya Rocket Range (69°N,16°E) on July 1–2 and 4–5, 2002. This paper investigates gravity waves in the mesosphere using falling spheres dropped from rockets and the Weber sodium lidar at the ALOMAR observatory. The vertical displacement of a sodium sporadic layer on July 5 showed great variability at periods from minutes to hours with an observed frequency spectral slope of −1.89. The 2 salvos had similar wave amplitudes at the mesopause, whereas Salvo 2 had stronger amplitudes in the lower atmosphere. The dominant wave period varied strongly with height, possibly due to wave breaking on the strong mean gradients or oblique propagation of wave packets. One long-period wave appeared to propagate vertically from 75–95 km with a reduction of its vertical wavelength consistent with the mean wind gradient, but it is unclear whether it was a single wave or a superposition of waves. *INDEX TERMS:* 0341 Atmospheric Composition and Structure: Middle atmosphere—constituent transport and chemistry (3334); 3332 Meteorology and Atmospheric Dynamics: Mesospheric dynamics; 3384 Meteorology and Atmospheric Dynamics: Waves and tides. **Citation:** Williams, B. P., D. C. Fritts, L. Wang, C. Y. She, J. D. Vance, F. J. Schmidlin, R. A. Goldberg, A. Müllemann, and F.-J. Lübken (2004), Gravity waves in the arctic mesosphere during the MaCWAVE/MIDAS summer rocket program, *Geophys. Res. Lett.*, *31*, L24S05, doi:10.1029/2004GL020049.

1. Introduction

[2] Atmospheric gravity waves are the primary source of variance at periods less than the inertial period (12.9 hr at 69°) in the middle and upper atmosphere. They generally propagate upward from sources in the lower atmosphere and deposit momentum and energy that drives a mean meridional circulation in the mesosphere and lower thermosphere, causing the polar mesopause to be cold in summer and warm in winter (see *Fritts and Alexander* [2003] for overview). The waves propagate horizontally and vertically, so large coordinated campaigns with multiple instruments are very useful to understand the propagation characteristics of the waves and their interaction with the mean state. Previous rocket campaigns addressing gravity wave dynamics included MAC/SINE, MAC/EPSILON [*Thrane*, 1990], and CADRE/MALTED [*Fritts et al.*, 1997].

[3] The MaCWAVE/MIDAS campaign in July 2002 combined rocket measurements, including falling spheres and neutral and plasma probes, launched from the Andøya Rocket Range in northern Norway with ground-based lidar and radar measurements from the nearby ALOMAR observatory. The campaign is described by *Goldberg et al.* [2003, 2004], with companion papers describing the tropospheric and stratospheric wave field [*Schöch et al.*, 2004], and mesospheric turbulence [*Rapp et al.*, 2004] and gradients [*Fritts et al.*, 2004]. We will concentrate here on gravity waves in the mesosphere and lower thermosphere observed by the Weber sodium lidar and falling spheres.

2. Instrumentation

[4] The Weber sodium lidar measures temperature, radial wind, and sodium density from roughly 85 to 100 km altitude by probing the Doppler width and Doppler shift of the atmospheric sodium resonance line [*She et al.*, 2002]. The Weber lidar uses a unique continuous-wave sum-frequency seed laser and an acousto-optic modulator to generate three highly stabilized seed frequencies at the sodium D_{2a} peak and ±630 MHz. The seed beam is combined with a pulsed YAG beam in the pulse dye amplifier to obtain roughly 1 W of pulsed power at 589 nm. The Weber lidar transmits two 0.5 W beams and receives the backscattered signal using the two 1.8 m diameter telescopes of the ALOMAR Rayleigh/Mie/Raman lidar. For the MaCWAVE/MIDAS campaign, the two beams were inclined 20° to the east and west of zenith, so meridional winds were not measured with the lidar. The east beam receiver had lower transmission, so we will use the west beam for the temperature and wind studies. We did not have enough signal from the east beam to calculate momentum flux. There was continuous sunlight throughout the campaign, so we used two sodium vapor magneto-optic Faraday filters as narrowband (2 pm FWHM) daytime filters to reject the solar background light. The vertical and temporal resolutions were 150 m and 1 min for the sodium density and 1 km, 1 hr or 4 km, 15 min for temperature and winds.

[5] During Salvo 1 on July 1–2 and Salvo 2 on July 4–5, 26 falling spheres were launched by Viper and Super-Loki rocket motors and tracked with a mobile, high-precision, C-band tracking radar to determine the horizontal winds from the horizontal motion and the atmospheric density from the vertical acceleration. The density can be related to

[1]Colorado Research Associates, a Division of Northwest Research Associates, Boulder, Colorado, USA.
[2]Also at Department of Physics, Colorado State University, Fort Collins, Colorado, USA.
[3]Department of Physics, Colorado State University, Fort Collins, Colorado, USA.
[4]NASA/GSFC/Wallops Flight Facility, Wallops Island, Virginia, USA.
[5]NASA/Goddard Space Flight Center, Greenbelt, Maryland, USA.
[6]Institute of Atmospheric Physics, Kühlungsborn, Germany.

0094-8276/04/2004GL020049

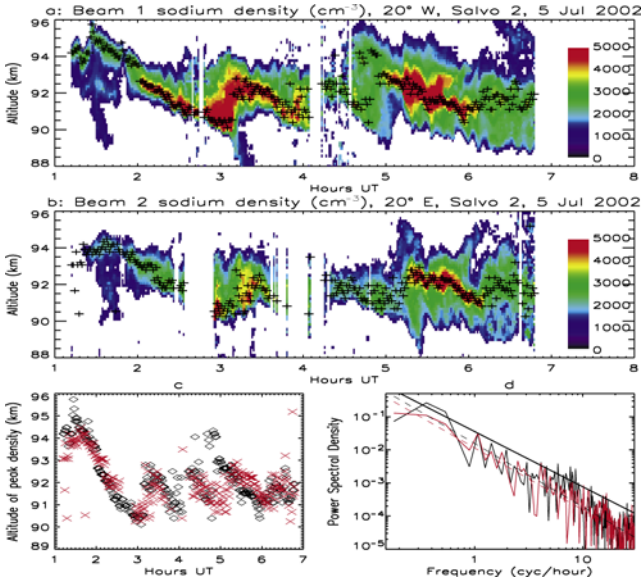

Figure 1. Closeup view of the sporadic sodium layer in Salvo 2. This shows the strong vertical motion due to waves and the similarities and differences between the 2 beams. The normal sodium layer has a density of roughly 1000 cm^{-3} and is not shown. The pluses mark the peak of the layer in a and b. The peak heights for both beams are compared in part c. In c and d, black (red) colors indicate beam 1 (2). Part d shows the power spectral density and the dashed lines are the best fit for each beam and the thin solid black is the expected 5/3 slope.

the temperature assuming hydrostatic equilibrium. Each sphere takes about 30 sec to fall through the mesopause region, so the vertical resolution was about 6 km (3 km) at 80 km (70 km) altitude [*Schmidlin et al.*, 1991]. Because of their higher apogees, we used the data only from 12 Viper rockets (6 for each salvo) for this study. The Viper falling spheres were about 40 km to the northwest of the rocket range and the nearby ALOMAR observatory and 30 km north of the west lidar beam at 90 km altitude.

[6] From the falling sphere measurements, we can determine the dominant gravity wave propagation direction, following the analysis by *Allen and Vincent* [1995]. Between 53 and 68 km, we determine the gravity wave perturbations by removing the semidiurnal tide by fitting the time series for each salvo and then subtracting mean profiles of winds and temperature smoothed with a 7.5 km low-pass filter. The analysis is rather sensitive to the tidal removal, so we only show results for the lower mesosphere where the inferred tides are small. The intrinsic frequency $\hat{\omega}$ is obtained from the axial ratio of the wind hodograph which is just $|\hat{\omega}/f|$ for a monochromatic wave, where f is the inertial frequency. The propagation direction is calculated using the Stokes parameters technique using u' and v' to define the wave direction and using T' to resolve the directional ambiguity.

3. Observations

[7] During both salvos, the sodium density measurements showed great variability at periods ranging from a few minutes to tens of hours, presumably due to gravity waves and tides. The sodium layer exhibited large changes in abundance and layer height with several sporadic layers and sharp bottom side gradients (Figure 1).

[8] During Salvo 2, the sodium density was typical for the summertime with a sharp sporadic sodium layer from ~1–7 UT on July 5. The region of the sporadic layer is shown in Figure 1 for both beams. We analyzed the vertical displacement of the peak of the sporadic layer as measured by the two Na lidar beams at 150 m and 1 min resolution over a 6 hr time period. This should be a good tracer for vertical motions as the vertical advection of the strong sodium density gradients should dominate the horizontal advection of Na density gradients, adiabatic compression/expansion, and any changes due to sodium chemistry. For periods greater than 1hr, the vertical displacements of the two beams (separated by 60–70 km horizontally at 90–100 km altitude) generally agreed well (see Figure 1c) suggesting that the displacements were caused by waves with large horizontal wavelengths moving the sporadic layers up and down. There are significant differences at higher frequencies and near 5 UT, which we believe are due to shorter horizontal wavelength waves.

[9] In Figure 1d, we show the observed frequency spectra of the vertical displacement of the sporadic layer peak. The spectra from the two beams were similar with an average slope of −1.89, which falls off slightly faster than the expected slope of −5/3. The vertical displacement spectrum should follow the temperature spectrum, rather than the vertical wind spectrum, as the displacement is the integral of the vertical wind in time. Past measurements of this slope have ranged from −1 to −2 [*Collins et al.*, 1994]. Since most of the power was at longer periods, the effect of Doppler shifting should be small, and the observed spectra

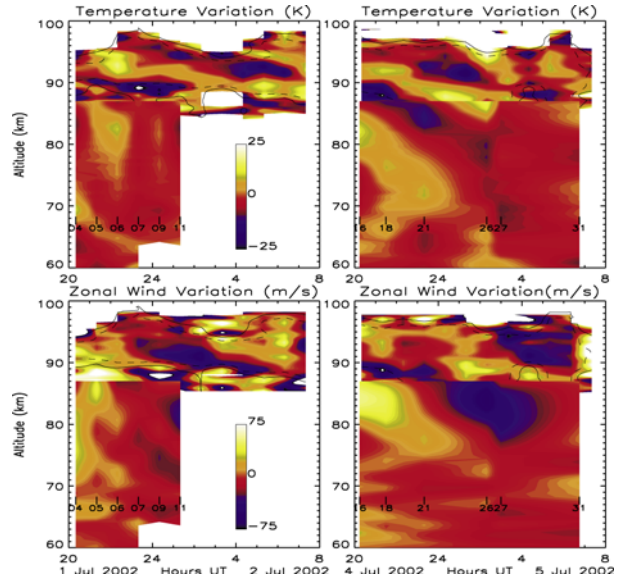

Figure 2. Temperature (top 2 panels) and wind (bottom 2 panels) variation about the salvo mean measured by the falling spheres and the sodium lidar for Salvo 1 (left) and Salvo 2 (right). The dashed and solid lines show the 10 K and 20 K error contours for temperature (25 and 50 m/s for wind). The falling sphere launches are marked by the short vertical lines and rocket numbers.

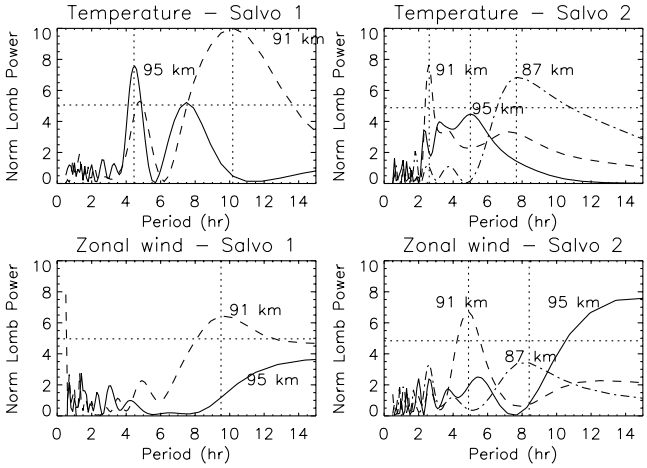

Figure 3. Lomb spectra for several altitudes for temperature (top 2 panels) and wind (bottom 2 panels) from the sodium lidar for Salvo 1 (left) and Salvo 2 (right). The horizontal dotted lines show the 30% significance level. The vertical lines mark the peak period for each spectrum.

presented here should resemble the intrinsic frequency spectra [*Fritts and VanZandt*, 1999].

[10] Temperature and zonal wind variations about the means are shown combining lidar and falling sphere data for each salvo in Figure 2. These show large wave perturbations generally with the downward phase progression expected for upward propagating waves. We will first discuss the dominant waves for Salvo 1 from both falling sphere and lidar data and then those for Salvo 2.

[11] The falling sphere data during Salvo 1 from 65–80 km showed waves with roughly 10-km vertical wavelength and 6-hr period in the zonal wind field. The temperature shows downward phase progressions between 60 and 70 km, and a long vertical wavelength signal from 70–85 km that is difficult to characterize due to the limited time sampling in the falling sphere data. In Figure 3, we show Lomb periodograms for temperature and zonal wind from the sodium lidar data. The properties of the dominant waves for each periodogram are shown in Table 1. The periodograms for Salvo 1 have peaks near 10 hours in temperature and zonal wind at 91 km. There is another significant peak at 4.5 hr at 91 and 95 km, but only in the temperature field.

[12] In Salvo 2, at 80 km the dominant wave has a roughly 12-hr period and a 25-km vertical wavelength. At 85 km, the falling sphere and lidar data both indicate a shorter vertical wavelength (about 12 km) and period (10 hr), in spite of the larger vertical smoothing in the falling sphere data At 90 km, the dominant vertical wavelength was 10 km and the period was closer to 8 hr. After 3 UT during Salvo 2, a 2-hr wave with a long vertical wavelength was dominant above 90 km in the temperature field. Similar variations were present in the sodium density as well. In Salvo 2, below 70-km altitude, the dominant waves had shorter vertical wavelengths of ~5 km. In Salvo 2, the temperature periodogram had peaks at 8 hr at 87 km, at 2.5 hr at 91 km, and 5 hr at 95 km. In Salvo 2, the zonal wind periodogram had peaks at 8 hr at 87 km, 5 hr at 91 km, and 15+ hr at 95 km. The dominant wave period changes rapidly with altitude and time, possibly due to enhanced wave breaking and large temperature, wind, and sodium density gradients in the upper mesosphere as discussed further below.

[13] In Table 1, we also show the potential energy per unit mass calculated from the temperature perturbation and kinetic energy per unit mass (*KE*) of the zonal wind perturbation. There was no systematic difference in the wave energies between the 2 salvos, in contrast to *Schöch et al.* [2004] which showed smaller than normal wave activity in the troposphere and stratosphere during Salvo 1, but much larger wave activity in Salvo 2. The falling sphere measurements in the lower mesosphere (see Figure 4) also showed higher wave amplitudes during Salvo 2, suggesting a change in the wave field below the mesopause. Rocket measurements indicated unusual enhanced turbulence from 72–82 km during both salvos, in addition to the more normal turbulent layer from 82–90 km [*Rapp et al.*, 2004]. This turbulence may have been due to wave breaking and *Rapp et al.* [2004] contend that the large wave amplitudes in the upper mesosphere were caused by the unusual background wind and temperature profiles rather than the wave source strength in the lower atmosphere. Salvo 1 also contained a very large positive temperature gradient at 89–91 km altitude of +40 K/km, which would have lead to enhanced wave breaking at those altitudes [*Fritts et al.*, 2004].

[14] Typically, at these latitudes, the semidiurnal tide has a larger amplitude than other tidal modes or gravity waves [*Hoffmann et al.*, 1999], but that was not the case during this campaign. During both salvos, there was very little power at periods greater than 10 hr, except for the zonal

Table 1. Dominant Wave Periods, Amplitudes, and Energies[a]

Salvo	Alt. (km)	T Per. (hr)	T Amp. (K)	U Per. (hr)	U Amp. (m/s)	U KE (J/kg)	N (s^{-1})	PE (J/kg)
1	91	10.2	7.7	9.5	21.7	240	0.029	280
1	95	4.5	9.0	19.2	10.9	59	0.025	280
2	87	7.7	8.9	8.4	18.8	180	0.028	340
2	91	2.6	7.1	4.9	12.8	82	0.027	200
2	95	3.4	4.4	15.4	19.5	190	0.026	72

[a]The kinetic energy was calculated from the zonal wind only.

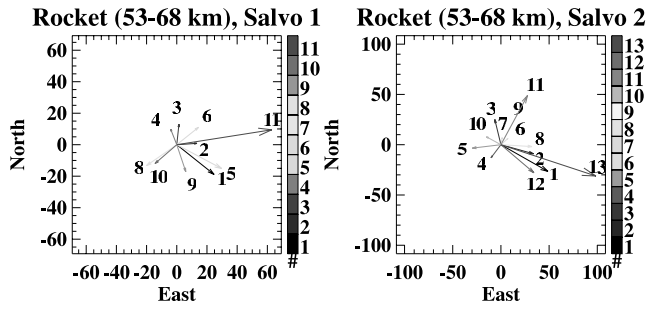

Figure 4. Horizontal wave propagation directions for mesosphere from 53–68 km. The falling spheres are numbered sequentially with Salvo 1 on 1–2 July 2002 on the left and Salvo 2 on 4–5 July 2002 on the right. The arrow direction gives the direction of mean horizontal wave propagation and the arrow length is proportional to kinetic energy density (J/kg).

wind at 95 km, but with only 12 hours of data, these tidal inferences are only suggestive.

[15] From the falling sphere measurements, we determined the dominant gravity wave propagation directions for 53–68 km altitude (Figure 4). There was a strong preference for eastward propagation in the 53–68 km altitude segment, consistent with filtering by the westward mean wind in the stratosphere and lower mesosphere [*Schöch et al.*, 2004]. The eastward waves had significantly higher kinetic energy densities than the westward propagating waves. Intrinsic periods calculated for each sounding ranged from 0.5–10 hr with most values in the range 1–4 hr. Vertical wavelengths varied from 6–10 km, covering much of the range allowed by the analysis procedure. The inferred dominant wave period changed from profile to profile, but we note that this quantity is highly uncertain if multiple waves were present. This is consistent, however, with the rapid changes with time of the periods of the waves evident in the sodium densities at higher altitudes (see Figure 1). There seemed to be many different wave packets propagating up through the atmosphere, each one dominant for one or two periods.

[16] The long-period wave that occurred between 80 and 90 km altitude during Salvo 2 showed reduction of its vertical wavelength as it propagated upward. The temperature lagged the zonal wind by a quarter of the period (see Figure 2), suggesting eastward propagation. The mean zonal wind during the salvo increased with altitude from 80 to 90 km [*Goldberg et al.*, 2004]. This would decrease $c - \overline{u}$, where c is the phase speed and $\overline{u}$ is the mean zonal wind, leading to a decrease in vertical wavelength, $\lambda_z \propto (c - \overline{u})/N$, with increasing altitude, consistent with the measurements. However, the apparent dominant period also decreased with altitude at the same time. This was not expected and it suggests that instead of a single wave, there may have been a superposition of different waves at different heights.

4. Conclusions

[17] This campaign made some of the most complete measurements of the atmosphere to date, with complete temperature and wind profiles from the ground to 100 km. Specific inferences of instability and turbulence arising from these motions are provided by *Fritts et al.* [2004] and *Rapp et al.* [2004]. The temperatures, zonal winds, and sodium densities measured by the Weber lidar are extremely variable, with strong wave perturbations at a variety of periods. The vertical displacement of the sporadic sodium layer on July 5 showed great variability at periods ranging from minutes to hours with general agreement between the 2 beams and with an observed frequency spectral slope of −1.89, similar to previous studies. Wave directions had an eastward bias in the lower mesosphere, consistent with filtering by mean winds lower down [*Schöch et al.*, 2004], with larger amplitudes in Salvo 2. These waves propagate largely upward into the mesopause region where their amplitudes are modified by the background profiles and wave breaking yielding roughly equivalent amplitudes during the 2 salvos in the mesopause region. We seem to have measured a number of different waves in the combined temperature and wind profiles that either break at different heights in the mesopause region as they interact with the large gradients present or that propagated obliquely through the lidar beam, coherent in the measurements for only one to two vertical wavelengths and one to two periods.

[18] **Acknowledgments.** The Weber Na lidar is a cooperative effort of the Colorado State University, CoRA/NWRA, the Leibniz-Institute of Atmospheric Physics, and the Andøya Rocket Range. This research was supported by AFOSR contracts F49620-00-C-0008 and F49620-03-C-0045, NASA contracts NAG5-02036 and NAS5-01075, NSF grants ATM0137555 and ATM0137354, and German BMBF grants 50OE9901 (ROMA) and 50OE9802 (MIDAS).

References

Allen, S., and R. A. Vincent (1995), Gravity wave activity in the lower atmosphere: Seasonal and latitudinal variations, *J. Geophys. Res.*, *100*, 1327–1350.

Collins, R. L., A. Nomura, and C. S. Gardner (1994), Gravity waves in the upper mesosphere over Antarctica: Lidar observations at the South Pole and Syowa, *J. Geophys. Res.*, *99*, 5475–5485.

Fritts, D. C., and M. J. Alexander (2003), Gravity dynamics and effects in the middle atmosphere, *Rev. Geophys.*, *41*(1), 1003, doi:10.1029/2001RG000106.

Fritts, D. C., and T. E. VanZandt (1999), Effects of Doppler shifting on the frequency spectra of atmospheric gravity waves, *J. Geophys. Res.*, *92*, 9723–9732.

Fritts, D. C., et al. (1997), Equatorial dynamics observed by rocket, radar, and satellite during the CADRE/MALTED campaign, 2, Mean and wave structures, coherence, and variability, *J. Geophys. Res.*, *102*, 26,191–26,216.

Fritts, D. C., B. P. Williams, C. Y. She, J. D. Vance, M. Rapp, F.-J. Lübken, A. Müllemann, F. J. Schmidlin, and R. A. Goldberg (2004), Observations of extreme temperature and wind gradients near the summer mesopause during the MaCWAVE/MIDAS rocket campaign, *Geophys. Res. Lett.*, *31*, L24S06, doi:10.1029/2003GL019389.

Goldberg, R. A., et al. (2003), The MaCWAVE program to study gravity wave forcing of the polar mesosphere during summer and winter, in *ESA Symposium on European Rocket and Balloon Programmes and Related Research: 11th ESA Symposium, Montreux, Switzerland, 24–28 May 1993*, edited by B. Kaldeich and E. J. Rolfe, pp. 345–350, Eur. Space Agency, Paris.

Goldberg, R. A., et al. (2004), The MaCWAVE/MIDAS rocket and ground-based measurements of polar summer dynamics: Overview and mean state structure, *Geophys. Res. Lett.*, *31*, L24S02, doi:10.1029/2004GL019411.

Hoffmann, P., W. Singer, and J. Bremer (1999), Mean seasonal and diurnal variations of PMSE and winds from 4 years of radar observations at ALOMAR, *Geophys. Res. Lett.*, *26*, 1525–1529.

Rapp, M., B. Strelnikov, A. Mllemann, F.-J. Lübken, and D. C. Fritts (2004), Turbulence measurements and implications for gravity wave dissipation during the MaCWAVE/MIDAS rocket program, *Geophys. Res. Lett.*, *31*, L24S07, doi:10.1029/2003GL019325.

Schmidlin, F. J., H. S. Lee, and W. Michel (1991), The inflatable sphere: A technique for the accurate measurement of middle atmosphere temperatures, *J. Geophys. Res.*, *96*, 22,673–22,682.

Schöch, A., G. Baumgarten, D. C. Fritts, P. Hoffmann, A. Serafimovich, L. Wang, P. Dalin, A. Mülleman, and F. J. Schmidlin (2004), Gravity waves in the troposphere and stratosphere during the MaCWAVE/MIDAS summer rocket program, *Geophys. Res. Lett.*, *31*, L24S04, doi:10.1029/2004GL019837.

She, C. Y., J. D. Vance, B. P. Williams, D. A. Krueger, H. Moosmuller, D. Gibson-Wilde, and D. C. Fritts (2002), Lidar studies of atmospheric dynamics near polar mesopause, *Eos Trans. AGU*, *83*, 289–293.

Thrane, E. V. (1990), Studies of middle atmosphere dynamics: The research projects Middle Atmosphere Co-operation/Summer in Northern Europe (MAC/SINE), and MAC/EPSILON, *J. Atmos. Terr. Phys.*, *52*, 815–825.

D. C. Fritts, L. Wang, and B. P. Williams, Colorado Research Associates, a division of Northwest Research Associates, 3380 Mitchell Lane, Boulder, CO 80301, USA. (biff@cora.nwra.com)

R. A. Goldberg, NASA/Goddard Space Flight Center, Greenbelt, MD 20771, USA.

F.-J. Lübken and A. Müllemann, Institute of Atmospheric Physics, D-18225 Kühlungsborn, Germany.

F. J. Schmidlin, NASA/GSFC/Wallops Flight Facility, Wallops Island, VA 23337, USA.

C. Y. She and J. D. Vance, Department of Physics, Colorado State University, Fort Collins, CO 80523, USA.